Evaluation of $I(V)$ curves in scanning tunneling spectroscopy of organic nanolayers

C. Wagner,* R. Franke, and T. Fritz
Institut für Angewandte Photophysik, Technische Universität Dresden, 01062 Dresden, Germany
(Received 23 January 2007; revised manuscript received 3 April 2007; published 21 June 2007)

We want to verify if the use of *scanning tunneling spectroscopy* (STS) evaluation methods developed for inorganic samples can be justified also for the case of organic nanolayers, or if modifications are necessary. This question arises since the traditional approaches are derived for the case of bulk samples and low voltages. Since an organic adsorbate on a substrate presents a sample with a more complex structure and is further characterized by a large gap in the eV range, the answer to this question is not *a priori* clear. After discussing relevant quantities, i.e., the sample *density of states* (DOS) and *local density of states*, we demonstrate the use of the simple and well-known model of a one-dimensional tunnel junction in Wentzel-Kramers-Brillouin approximation in order to calculate the sample DOS for several STS results from literature dealing with ultrathin organic layers. In a subsequent discussion, we conclude that the model is applicable to the orbital-mediated tunneling process "through" organic molecules and that it can be used to evaluate such STS measurements. Emanating from an estimation of the tip-sample distance, the possibility of detecting electronic states below the *highest occupied molecular orbital* in STS is discussed. With several examples, we illustrate a weakness of the normalized differential conductivity as a method of STS $I(V)$ curve evaluation and propose a new normalization algorithm as a solution to the problem.

DOI: 10.1103/PhysRevB.75.235432 PACS number(s): 73.43.Jn, 73.20.At, 73.43.Cd

I. INTRODUCTION

The invention of the scanning tunneling microscope (STM) in 1982 by Binnig *et al.*[1] opened up the possibility to investigate not only the topography of a conducting sample at atomic resolution but also the electronic properties of such a sample at a comparable lateral resolution. For this purpose, scanning tunneling spectroscopy (STS) is used to obtain information about the density of electronic states (DOS) of the surface.

Bare metal and semiconductor surfaces have already been studied intensively since the invention of the STM. However, today a significant part of the STM and/or STS results published deals with the investigation of ultrathin organic adsorbate layers. The opportunity to tailor and control organic molecules for special purposes opens up a new field of prospective applications. The use of such molecules in organic light-emitting diodes[2,3] or organic solar cells[4,5] as well as in future devices generally referred to as "molecular electronics"[6,7] requires the investigation and understanding of the electronic properties of organic adsorbates, especially on metal surfaces as they are inevitably present in any electronic device. Scanning tunneling spectroscopy is a suitable method to study these properties as it provides information on both the empty and the filled electronic states in just one measurement. Using the ultrahigh-resolution capabilities of STM, this information can, in principle, be obtained on a very local scale. However, here we do not discuss the spatial resolution, but concentrate on the question of how can one reliably extract the energetic position of the molecular states, as those will influence the device performance to a large extent. Among those electronic states, undoubtedly the highest occupied molecular orbital (HOMO) and the lowest unoccupied molecular orbital (LUMO) play a major role since it is those orbitals which define the electronic gap. Nonetheless, in general, molecules feature many closely neighbored but still well-separated occupied and unoccupied states right below the HOMO and above the LUMO.[8] Several of them are accessible in STS measurements with a typical voltage range between ±2.5 V.[9,10] It is of general interest to identify the energetic positions of those states as well, as this can provide valuable input to any theoretical description of the tunneling process through organic adsorbates.

If the $I(V)$ curve is not discussed phenomenologically in terms of a conductance gap, there are two different approaches to the interpretation of STS spectra in literature: Either the differential conductivity dI/dV or the normalized differential conductivity $(dI/dV)/(I/V)$ is used, following the argumentation of Tersoff and Hamann[11] or Stroscio *et al.*,[12] respectively. Besides the fact that two dissimilar methods of interpretation represent an undesirable degree of freedom, both methods have originally been proposed for the interpretation of STS results on bulk inorganic samples. The use of these methods on organic adsorbates therefore evokes two problems: On the one hand, the sample structure is more complex if an adsorbate is present which may affect the tunneling process. On the other hand, a rather large tunneling voltage, compared to STS on inorganic samples, is necessary to probe the molecular resonances. These differences from the inorganic case motivate this revision of the evaluation of STS measurements on organics.

Quite clearly, this has to involve a model of the tunneling process. Besides the very sophisticated quantum chemistry models already established,[13,14] some simple models are being discussed in literature. Those simple models have the clear advantages that they can promote a deeper insight in the tunneling process and that they might be used in the daily work of an experimentalist to analyze the measured data.[15,16] Still, the fundamental question whether the same models can be used to describe the tunneling between a metal tip and an inorganic sample on the one hand and the orbital-mediated tunneling into a substrate covered by organic molecules on

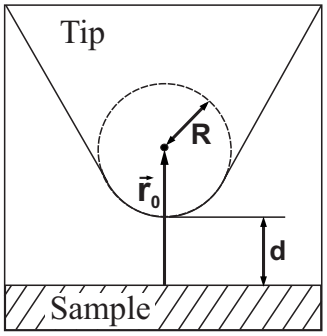

FIG. 1. Schematic picture of the tunneling geometry (Ref. 11). The tip is assumed locally spherical with a radius R.

the other hand has found only little attention in literature up to now. One of the most widely discussed simple models is the one-dimensional (1D) model of a tunnel junction that makes use of the Wentzel-Kramers-Brillouin (WKB) approximation[17] and has first been suggested by Selloni *et al.*[18] and Lang.[19]

Here, we discuss the issues of applicability of this 1D WKB model to the case of orbital-mediated tunneling through a thin molecular layer on a metal substrate. For that purpose, we use the complete 1D WKB model to calculate the DOS, introducing a new approach to do so. Then, we compare the DOS obtained from the full model with the known approximate approaches, i.e., the differential conductivity (dc) and the normalized differential conductivity (ndc). Advantages and disadvantages of both quantities are highlighted. Here, we also deal with the question whether occupied sample states below the HOMO can be probed by STS at all, or whether their contribution is too weak to be noticed. Exemplarily, four different STS measurements from literature are discussed, including examples which exhibit negative differential resistance (NDR) effects, since the NDR phenomenon is thought to be a valuable benchmark to check the significance of any model. While the applicability of the model is presumed at first, an assessment of the resulting DOS and of additional relevant parameters will later confirm or negate this assumption.

However, to put things into the right perspective, we first summarize the exact meaning of the terms DOS and local density of states (LDOS) and demonstrate the relation to quantities measured in STS, as this is an indispensable prerequisite for our calculations with the 1D WKB model.

II. CALCULATING THE CURRENT IN A TUNNEL JUNCTION

A theoretical basis for a general treatment of the tunneling process in a STM is given by Bardeen, known as the transfer Hamiltonian approach.[20,21] Tersoff and Hamann applied this approach to a model of a flat surface and a spherical tip with an atomic s-orbital symmetry (Fig. 1), thus creating the first quantitative model for the tunneling current in a STM.[11] As a result, one gets the following expression for the tunneling current I in the limit of zero temperature and very low voltages:[22]

$$I = 32\pi^3\hbar^{-1}e^2V\Phi^2\rho_t(E_F)R^2\kappa^{-4}e^{2\kappa R}\sum_\nu |\Psi_\nu(\vec{r}_0)|^2\delta(E_\nu - E_F). \tag{1}$$

In this equation, I depends on the average work function $\Phi=(\Phi_t+\Phi_s)/2$ of tip and sample and on the density of states ρ_t of the tip at the Fermi level. The sample properties are represented by the value of the sample wave functions Ψ_ν with an energy E_ν at the center of curvature $\vec{r}_0$ of the tip (Fig. 1), constituting the LDOS. The LDOS thus represents the charge density per unit energy at E_F at a certain point above the surface.[23] From Eq. (1), one can derive a first important relation between the LDOS and the tunneling current $I(V)$ at very small bias, i.e., around E_F:

$$dI/dV \propto \mathrm{LDOS}(E_F). \tag{2}$$

For the discussion of $I(V)$ dependencies in STS measurements on organics, where the energy gap between the HOMO and the LUMO typically exceeds 1 eV, the limit of $V\approx 0$ is obviously inappropriate. If a sizable bias voltage is applied, it is necessary to introduce a voltage dependence of (at least) the sample wave functions: $\Psi_\nu=\Psi_\nu(\vec{r}_0,V)$. An appropriate description of the tunneling process would therefore require the calculation of the sample wave functions in the electrostatic potential created between the sample and the tip, which is extremely complicated, especially if the tip shape is not known precisely.[24] Thus, such an approach is not very useful for a general discussion of STS measurements. Instead, the standard way to introduce a voltage dependence is to use the model of a one-dimensional tunnel junction in the WKB approximation. The model includes a number of approximations such as the neglect of image potential effects and inelastic tunneling as well as the limit of zero temperature. However, by comparing the results of the full transfer Hamiltonian calculation to the 1D WKB model in a bias voltage range of ±2 V, Lang found a good agreement between both methods and concluded that "…The simple model provides a good account of the qualitative features of the results of the full calculation…."[19]

The respective equations express the tunneling current as an integral over the density of states of the tip and the sample and the barrier transmission function T which results from the WKB approximation, assuming a trapezoidal barrier:

$$I(d,V) \cong \frac{A\pi e\hbar^3}{2m^2}\int_0^{eV} T(d,V,E)\rho_s(E)\rho_t(E-eV)dE, \tag{3}$$

with

$$T(d,\Phi_{s,t},V,E) \cong \exp\left[-2(d+R)\frac{2}{3}\sqrt{\frac{2m}{\hbar^2}} \times\left(\frac{(\Phi_t - E + eV)^{3/2} - (\Phi_s - E)^{3/2}}{\Phi_t - \Phi_s + eV}\right)\right]. \tag{4}$$

The quantities in these equations are illustrated in Figs. 1 and 2.

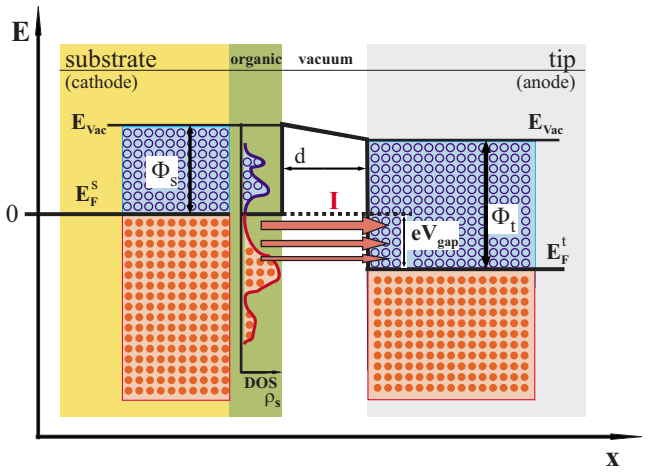

FIG. 2. (Color online) The model of a one-dimensional tunnel junction with a trapezoidal barrier.

To put this 1D WKB model into perspective, a short comparison to the Tersoff-Hamann model shall be made: The Tersoff-Hamann model aims at a more accurate description by considering individual sample wave functions, but gives no answer on how the value $|\Psi_\nu|$ at $\vec{r}_0$ should be calculated and how it changes with an applied voltage. The 1D WKB model circumvents these questions by not dealing with the wave functions directly. Instead, a density of electronic states is assumed where the individuality is reduced to a dependency on the energy E of each state. The dependencies on E and on V are then combined in the transmission function T which can be seen as a measure for the charge density of each state that reaches r_0. Thus, the quantity

$$\rho_s(E)T(r_0,V,E) \overset{1D\ WKB}{\equiv} \mathrm{LDOS}(E) \tag{5}$$

is a generalized LDOS at r_0 in terms of the Tersoff-Hamann model.[25] From this relation, the fundamental difference between the DOS ρ_s and the LDOS of the sample becomes immediately clear. Consequently, one has to clearly distinguish between the two terms in general, notwithstanding that cases exist where LDOS and DOS bear a close resemblance to each other.

Calculating the derivative of Eq. (3) with respect to V results in three terms:

$$\frac{dI(d,V)}{dV} \cong A\left[eT(d,V,E)\rho_s(E)\rho_t(E-eV)|_{E=eV} + \int_0^{eV} T(d,V,E)\rho_s(E)\frac{d\rho_t(E-eV)}{dV}dE + \int_0^{eV} \frac{dT(d,V,E)}{dV}\rho_s(E)\rho_t(E-eV)dE \right]. \tag{6}$$

From substituting Eq. (5) into Eq. (6), it is evident that only for very small biases the statement $dI/dV \propto \mathrm{LDOS}$ holds, in agreement with the Tersoff-Hamann model (see above). However, for increasing biases, this relation becomes less and lesser valid, simply due to the explicit voltage dependency of T, so that the other two terms in Eq. (6) will not vanish.[26] From this, we can already conclude that the relation

$$\frac{dI}{dV} \propto \rho_s(eV)T(d,V,eV) \equiv \mathrm{LDOS}(eV) \tag{7}$$

is only an approximate one. In addition, we like to note that the restriction to small biases leads directly to the assumption of a constant T and a constant ρ_t, and therefore one can approximately write

$$\frac{dI}{dV} \propto \rho_s(eV) \equiv \mathrm{DOS}(eV) \tag{8}$$

by the same token. Combining Eqs. (8) and (2), one comes to the conclusion that

$$\frac{dI}{dV} \propto \mathrm{DOS} \propto \mathrm{LDOS}, \tag{9}$$

which explains why both quantities are mixed up frequently when discussing STS measurements, ignoring the fact that Eq. (9) is only valid for small voltages.

The best and most convincing example to demonstrate the nonproportionality between dI/dV and the LDOS is the observation of an NDR, an effect that occurs especially in STS measurements on organic molecules which are separated from the metal substrate by a thin insulating layer.[10,27] In the respective bias voltage region the current drops, although the voltage is increased. Consequently, the differential conductivity dI/dV becomes negative, which cannot be the case for the DOS the LDOS, thus rendering $dI/dV \propto \mathrm{LDOS}$ and $dI/dV \propto \mathrm{DOS}$ invalid. The NDR effect can, on the other hand, easily be explained by the full 1D WKB model as will be shown in Sec. III B 1.

III. EXTRACTION OF THE DOS FROM STS MEASUREMENTS BY MEANS OF THE 1D WKB MODEL

From the previous discussion of the 1D WKB model, it became obvious that the LDOS depends on the respective energy, the tip-sample distance, and the applied bias voltage. On the other hand, the sample DOS $\rho_s(E)$ depends exclusively on the energy. When performing tunneling spectroscopy at a constant tip-sample separation, there is only one free variable, the bias voltage, and thus the quantity obtained from the measurement should also depend on only one variable. Moreover, as it has been pointed out already in the Introduction, using STS as the material characterization method, it is indeed the DOS that one should be interested in. While a significant number of publications use the 1D WKB model for the forward calculation of $I(V)$ curves, plugging in assumed tip and sample DOS distributions $\rho_t(E)$ and $\rho_s(E)$,[10,19,26] we will demonstrate here that one can invert the direction of calculation and use the model to directly calculate the DOS from measured $I(V)$ curves as a direct evaluation method.[28]

In the following part, we will briefly explain the method used and subsequently show the results for four examples of STS measurements from literature.

A. Solving the integral equation

The goal to calculate the sample DOS $\rho_s(E)$ (in terms of the 1D WKB model) from the STS $I(V)$ curve requires solving Eq. (3), which is a Volterra integral equation of the first kind. Although there is no analytical solution for this particular equation, it can be solved numerically, in principle, to any required accuracy. A simple but efficient method is to split up the $I(V)$ curve into a positive and a negative voltage part and to replace the integral by a numerical quadrature. For this purpose and for each polarity separately, the interval $[0, V_{max}]$ is divided into N smaller intervals of width ΔV and respective voltage steps $v_i = i\Delta V$. The values for ρ_s at these points are $P_i^s := \rho_s(ev_i)$ and equivalently $I_i := I(v_i)$.

Then, the integral can be approximated by a sum:

$$I_j = Ce\Delta V \sum_{i=0}^{j-1} T(d, \Phi_{s,t}, v_j, ev_i)\rho_t(v_j, ev_i)P_i^s. \tag{10}$$

The integral kernel $T(d, \Phi_{s,t}, v_j, ev_i)\rho_t(v_j, ev_i)$ consists of two physical quantities, the transmission function T which is given by Eq. (4) and the energy dependent tip DOS ρ_t. As the latter one is not known in most cases without further assumptions, only the product of tip and sample DOS can be calculated.

Since a flat tip DOS is assumed in most published STS results anyway,[29] we will follow this assumption here, treating ρ_t as a constant from now on and merging it with the prefactor C. The then unnecessary index s of P_i^s can be removed, i.e., the expression "DOS" will refer from now on always to the samples DOS, and we obtain

$$I_j = Ce\Delta V \sum_{i=0}^{j-1} T(d, \Phi_{s,t}, v_j, ev_i)P_i. \tag{11}$$

As the prefactor C contains the unknown value of the constant tip DOS, we can, without loss of generality, set the entire expression $Ce\Delta V$ equal to unity. No absolute value for the DOS can be obtained this way, i.e., the results are on an arbitrary scale. If we denote the $N \times N$ coefficients $T(d, \Phi_{s,t}, v_j, ev_i)$ as a matrix $\mathbf{T}^N$ with elements T_{ji} and equivalently define $\mathbf{I}^N = (I_1, \ldots, I_N)^\mathsf{T}$ and $\mathbf{P}^N = (P_0, \ldots, P_{N-1})^\mathsf{T}$, Eq. (11) can be written in matrix notation[30] as

$$\mathbf{I}^N = \mathbf{T}^N \mathbf{P}^N. \tag{12}$$

This system of linear equations can, in principle, be solved by Gaussian elimination. As $\mathbf{T}^N$ is, however, a lower-triangular matrix, the effort is reduced to a sequential calculation of the values P_j by following the iterative rule

$$P_j = \left[I_{j+1} - \sum_{i=0}^{j-1} T_{j+1,i} P_i \right] \Big/ T_{j+1,j}, \tag{13}$$

with

$$P_0 = I_1 / T_{1,0}.$$

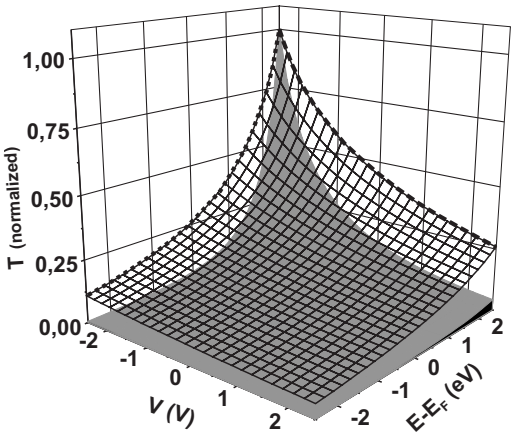

FIG. 3. Displayed is the normalized transmission function $T(d, \Phi_{s,t}, V, E)$ [Eq. (4)] for $\Phi_s = \Phi_t = 5$ eV and two different tip-sample distances: $d = 3.5$ Å (solid gray) and $d = 1.5$ Å (transparent mesh). The profiles of two cuts normal to the E-V plane are marked for $d = 1.5$ Å: $T(V = \text{const}, E)$ (dotted line) and $T(V, E = \text{const})$ (dashed line).

At least two different methods exist to calculate the coefficients T_{ji}. While the simplest approach is to set $T_{ji} = T(d, \Phi_{s,t}, v_j, ev_i)$, we have used the midpoint method as recommended by Linz and set $T_{ji} = T(d, \Phi_{s,t}, v_j, e(v_i + \Delta V/2))$.[31]

As the $I(V)$ curve resulting from an STS measurement is already discretized in the form of a list of (I, V) pairs, the voltage steps v_i and thus ΔV are given parameters. However, for the practical evaluation of Eq. (13), it is necessary to divide the list into two subsets as mentioned above. Then, the index j in Eq. (13) runs from 1 to $N_+ - 1$ or $N_- - 1$, respectively.

Advantageously, the computational effort for the DOS calculation proposed here is negligible on today's desktop computers, even if performed for a large set of STS $I(V)$ spectra. As solving an integral equation is involved, the calculation is rather noise sensitive. When dealing with very noisy $I(V)$ curves, a smoothing prior to the calculation might therefore be recommendable.

Finally, we note that the two other free variables, the tip-sample separation d and the average work function Φ, can alter the result of the calculation due to their influence on T and must therefore be discussed separately. This will be done in the next part at hand of an analytical example.

B. Influence of d and Φ on the result of the calculation: The role of the slope of T

1. Dependency of T on E, V, d, and Φ

The two free variables which have an influence on the evaluation of $I(V)$ curves [as we will call the calculation of the sample DOS by solving Eq. (12)] are the tip-sample distance d and the work functions Φ_s and Φ_t, in other words, the width and height of the tunneling barrier which influence the transmission probability. To illustrate this effect, Fig. 3 shows T as a normalized function of E and V for two differ-

ent tip-sample distances d. As constant prefactors have already been disregarded in the derivation of Eq. (12), the absolute value of T is not of interest anymore, but only the ratio between values of T for different points (E,V); in other words, the slope of T has to be considered. It is clearly visible in Fig. 3 that the overall slope increases with increasing tip-sample distance while it decreases for a higher value of $\Phi_{s,t}$ [not shown, compare Eq. (4)].

The discussion on how the recovery of ρ is influenced by the slope of T will, for the sake of clarity, be preceded by an illustration of the general impact of the transmission function on the tunneling current. We will therefore discuss two cases which can be associated with either the dashed or dotted thick line in Fig. 3 (note that the argumentation given here is again only valid for the case of a constant tip DOS).

Dashed line in Fig. 3. The tunneling current carried by electrons in a state X with an energy $E_F<E_x<E_F+eV$, $V>0$, decreases with increasing voltage due to the decreasing tunneling probability: $dI_x/dV<0$. However, for negative voltages and $E_F>E_x>E_F-e|V|$, $V<0$, the respective current increases with increasing negative voltage: $dI_x/dV>0$. This asymmetry with respect to $V=0$ includes the possibility of a decrease of the entire tunneling current with increasing voltage for positive bias polarity, while such a NDR effect can be excluded for negative bias.

Dotted line in Fig. 3. For constant bias, the tunneling probability for electrons decreases quasiexponentially with its energy. This does not necessarily apply also to the respective contribution to the tunneling current which is weighted by the number of electrons at each energy (the DOS). The small tunneling probability for electrons in low-energy states means, however, that a large proportion of the increase in the current with increasing negative voltage can be attributed to the effect described in the dashed line case above and not to the current through states at $E=E_F-e|V|$. To what extent these states contribute to the current nevertheless will be discussed for real experiments in Sec. IV C.

2. Choice of Φ and d for the evaluation procedure

From the discussion in the last part, we can conclude that the evaluation of experimental $I(V)$ curves by means of Eq. (12) requires the choice of specific values for d and $\Phi_{s,t}$ and thus for the slope of T. If, as in most cases, these values have not been measured in a separate experiment, they have to be estimated. Here, we analyze to what extent a recovered DOS curve in itself allows to determine those values.

As both parameters d and $\Phi_{s,t}$ have a comparable (but inverse) influence on the slope of T, it is, as a matter of fact, impossible to specify both values independently.[32] [An approach to estimate d and $\Phi_{s,t}$ from experimental $I(V)$ curves is given by Rosink *et al.* for the case of a flat tip and sample DOS.[16]] Therefore, we decide to simplify the discussion by keeping $\Phi=\Phi_s=\Phi_t$ constant at the reasonable value of 5 eV and discussing the DOS recovery exclusively in dependency on d.

Thereby, the argumentation given in the previous part is the basis for the following analysis, where we discuss two scenarios, one for positive and one for negative bias polarity, in order to define rules for the determination of d.

First scenario: Unoccupied DOS. A potential NDR effect at positive bias can be explained by a rise of the tunneling barrier with increasing voltage. This rise and, therefore also the NDR effect, increase with increasing tip-sample distance (see dashed line in Fig. 3). If an $I(V)$ curve with a NDR is evaluated and the chosen value for d is too low, the calculated rise of the barrier and thus the decrease of $I(V)$ are weaker than in the measurement. To compensate for that and to generate a stronger decrease of the current, a negative value for ρ is obtained in the NDR region.[33] The (obvious) demand for a positive DOS thus imposes a lower bound for d, if a NDR effect has been observed.

Second scenario: Occupied DOS. For negative bias, the current inevitably increases with increasing negative voltage. If, in the evaluation of an $I(V)$ curve, the value for d is too high, this effect is overestimated. To compensate for that and to artificially decrease the current to the value measured, parts of the DOS below E_F are calculated to be negative. In this case, the demand for a positive DOS imposes an upper bound for d.

Without any additional information, the value for d which should be used to evaluate a given $I(V)$ curve cannot be determined more precisely than within the limits of the upper and the (potentially existing) lower bound.

To illustrate the influence of different tip-sample distances on the evaluation of $I(V)$ curves, we choose an analytical example. In a first step a model DOS curve is created, which nevertheless exhibits general properties of a real molecular DOS, namely, well-separated and broadened resonances. Afterward, the STS experiment for $d=5$ Å, $\Phi=5$ eV is simulated by calculating an $I(V)$ curve with Eqs. (3) and (4) [Fig. 4(a)]. In a second step, the resulting $I(V)$ curve is evaluated by means of Eq. (12). This is done not only for the correct value of $d=5$ Å but also for $d=3$ Å and $d=6$ Å, thus demonstrating the effect described above by showing that parts of the calculated DOS at positive or negative bias become negative [Fig. 4(b)]. In this analytical example, the upper and lower bounds for d have almost the same value of about 5 Å, leaving only this correct value of 5 Å as an option. However, as we will show subsequently, this is not necessarily the case in the evaluation of real STS measurements.

To complete the discussion of the results given in Fig. 4(b), we would like to point out that, on the one hand, almost no shift of the peak positions between the dI/dV plot and the three DOS curves can be observed, but on the other hand, the relative height of the peaks is strongly affected by the tip-sample distance chosen. By the same token, we like to emphasize that if the usual approximation $dI/dV \propto \mathrm{DOS}$ [Eq. (9)] is chosen, the occupied states appear with strongly decreased intensity.

IV. PRACTICAL APPLICATION OF THE 1D WKB MODEL

A. Calculation of the sample DOS for experimental $I(V)$ curves

Since we have set up rules to identify the maximum range for the tip-sample distance from an $I(V)$ curve given, we can now continue by analyzing and evaluating $I(V)$ curves from real STS experiments on organic thin films.

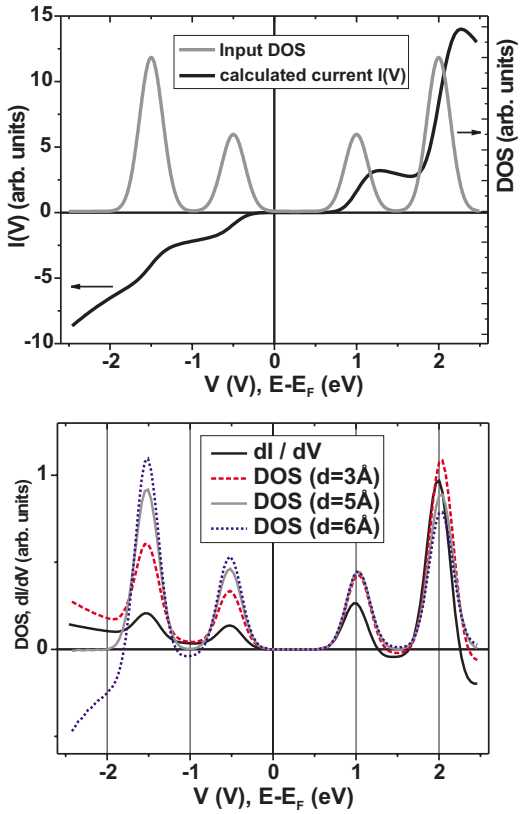

FIG. 4. (Color online) (a) Shown is a model DOS curve with four Gaussians as representations of molecular resonances and the respective $I(V)$ curve calculated by means of Eqs. (3) and (4) for a flat tip DOS, $d=5$ Å and $\Phi=5$ eV. (b) This graph shows the results of different evaluations of the $I(V)$ curve displayed in (a). Compared are the dI/dV plot and the sample DOS ρ obtained by solving Eq. (12) for a flat tip DOS, $\Phi=5$ eV, and three different tip-sample distances d. We would like to point out that the dI/dV curve equals the DOS curve for $d=0$ Å.

The goal to find a unique DOS curve belonging to an STS measurement is opposed by the uncertainty in the determination of d. As even comparably small variations in d lead to strong changes in the relative heights of the DOS peaks [Fig. 4(b)], one should not expect the relative peak heights in the examples discussed in this section to be an accurate representation of the true sample DOS peak heights in the experiment, although the complete 1D WKB model and not only the differential conductivity [Eq. (9)] is used for the calculation.

The applicability of the 1D WKB model will now be analyzed considering two criteria.

(1) Are the values found for the upper and lower bounds of the tip-sample separation reasonable if compared to experimental findings?

(2) Is the DOS curve obtained for a value d within these bounds physically meaningful?

The discussion of the second criterion will be based on the interpretation given in the respective publications.

We use the 1D WKB model to calculate the sample DOS for four different STS measurements from literature. If only the differential conductivity dI/dV is given in the publications, the respective $I(V)$ curves are obtained by integration (not shown here). We focus especially on reports demonstrating negative differential resistance, because this is the phenomenon for which the 1D WKB model is frequently used as an explanation and which is therefore most useful in demonstrating the functionality of our calculation. A second reason is given by the fact that for measurements with NDR, an upper and a lower bound for d can be found.

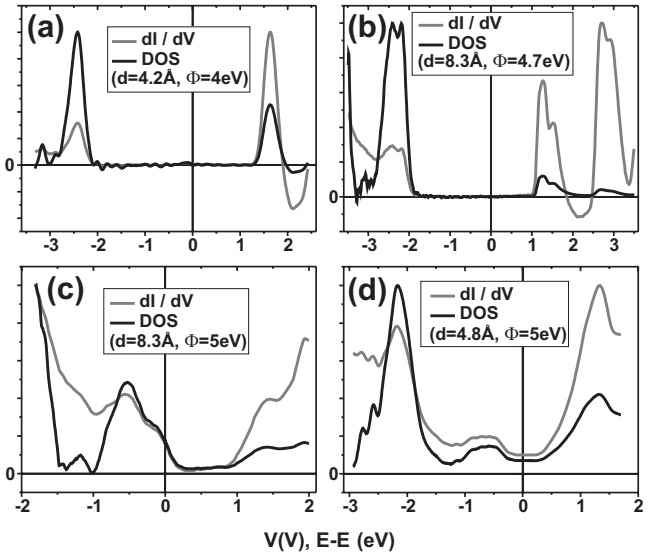

FIG. 5. Results of an evaluation with the 1D WKB model: (a) Repp *et al.* (Ref. 27), (b) Grobis *et al.* (Ref. 10), (c) Barlow *et al.* (Ref. 34), and (d) Tsiper *et al.* (Ref. 35). Displayed is dI/dV versus the DOS from the calculation.

A reasonable value of 5 eV is chosen for $\Phi_{s,t}$ [except for cases (a) and (b) in Fig. 5, where a value for Φ_s of 4 or 4.7 eV, respectively, was assumed by the authors themselves[10,27]]. It is important to mention that a guess for Φ that deviates by a few 100 meV from the real value has only a weak influence on the values of the upper and lower bounds for d and none at all on our conclusions. To avoid ambiguity, we consequently show the DOS which was calculated using the upper limit for d, although this is not necessarily a good guess as will become clear later. The reason for this choice lies in the fact that the upper limit is given in all four cases, while a lower limit can only be specified if an NDR is observed.

The results of the evaluation with the 1D WKB model which are displayed in Fig. 5 are summarized here briefly.

(a) The first example in Fig. 5 shows the evaluation of an STS measurement from Repp *et al.* for individual pentacene molecules on an ultrathin NaCl layer on Cu(111).[27] A NDR effect was observed and explained by the decoupling of metal substrate and molecules due to the NaCl layer. In this example, the upper and lower limits for d obtained from the calculation do overlap. As can be seen in Fig. 5, the DOS in the NDR region is slightly negative if calculated for the upper limit of $d=4.2$ Å. The lower value for d, for which the NDR effect can be explained properly by the model is, in a clear contradiction, at approximately 10 Å.

(b) The second example shows the evaluation of an STS measurement on a C_{60} double layer on Au(111) from Grobis

et al.[10] The separation of the second monolayer from the substrate leads again to an NDR effect. The upper limit for d is 8.3 Å, while the lower limit is 3.5 Å. A strong asymmetry in the density of occupied and unoccupied states is visible, while the asymmetry in the dI/dV plot is weaker.

(c) The third example shows a STS result for a CoPc layer on Au(111) from Barlow *et al.*[34] As no NDR effect was observed, no lower bound for d can be determined. Figure 5 shows the DOS for the upper bound $d=8.3$ Å. Again, a high asymmetry in the height of the peaks in the density of filled and empty states is visible for this particular value of d.

(d) The last example, an STS investigation by Tsiper *et al.*, shows the result for a monolayer of 3,4,9,10–perylene-3,4,9,10–tetracarboxylicdianhydrid (PTCDA) on Au(111).[35] The upper bound for the tip-sample distance was found to be $d=4.8$ Å. The asymmetry in the relative height of the HOMO and LUMO peak in the DOS is small compared to those in examples (b) and (c).

Apparently, in all calculations the density of the occupied states is higher than those of the unoccupied states. This will be discussed in more detail in the next section.

B. Discussion of results and comparison to the differential conductivity

The results shown in Fig. 5 allow us to draw a number of reliable as well as speculative conclusions. Among the former ones is the fact that the upper and, if detectable, the lower bound for the tip-sample distance have a physically realistic value [a value of 4 Å has been found for PTCDA on S-GaAs(001) (Ref. 36)]. Furthermore, the position of the DOS peaks is virtually identical to the position of the respective peaks in the dI/dV curve for all examples shown. This is important as it means that the interpretation of the dI/dV peak positions given in the respective publications remains valid also for the calculated DOS. Obviously, the asymmetric transmission function T is barely influencing the positions of the peaks, while a strong influence on the relative height of the peaks is evident. In all examples, the calculated density of occupied states is higher than the density of unoccupied states, whereas a comparably weak opposite trend is visible in the respective differential conductivity plots. The strength of the asymmetry found in the calculated DOS curves is directly related to the tip-sample distance used: A comparably large value for d leads to a strong slope of T and thus to a pronounced asymmetry in the DOS.

It is, however, dangerous to discuss the peak heights in the DOS as well as in the dI/dV plots without further considerations. Constraints are given by the fact that the peak heights can be influenced by other effects than the 1D WKB transmission function alone, namely, by the specific geometry of the involved orbitals which may not be entirely consistent with the 1D WKB model and thus result in transmission factors which are specific for each orbital.[13] A second aspect is a degeneracy of orbitals and the so-called "level bunching," both resulting in a high density of states in a small energy region that cannot be resolved by STS and thus appears as one large peak (see, for example, Ref. 37 for electron spectroscopy results). For these very reasons, a DOS

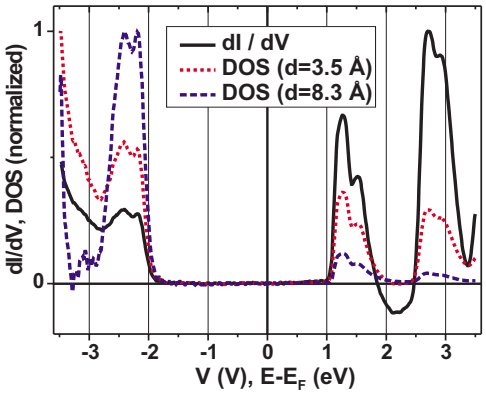

FIG. 6. (Color online) Displayed is a comparison of the dI/dV plot belonging to the STS measurement by Grobis *et al.* (Ref. 10) to two different DOS curves calculated for the upper and lower bounds of the tip-sample distance d with $\Phi=4.7$ eV.

can contain peaks of quite different height. As we see it, however, there is no physical reason for the general suppression of unoccupied states as it is present in all examples in Fig. 5; we rather attribute this effect to a value of d chosen too high for the calculation.

With these qualifications, the asymmetry in the dI/dV as well as in the DOS curves can be explained consistently if one assumes the value of $d=0$ and thus $T=$const [resulting in Eq. (9)] to be (definitely) too small and, on the other hand, the value of the upper bound $d=d_{max}$ to overestimate the real tip-sample distance in the experiments. To illustrate this consideration, Fig. 6 shows again the STS results of Grobis *et al.* [Fig. 5(b)] in comparison to the DOS curve for the upper and the lower limit for d. The DOS calculated for the lower limit $d=3.5$ Å exhibits a better balance in the height of the occupied and unoccupied DOS peaks than the dI/dV plot or the DOS curve for $d=8.3$ Å, respectively. Recapitulating, one has to state that with the considerations mentioned above, a value of less than 5 Å for the tip-sample distance represents a much better estimation than the calculated upper bound of 8.3 Å in examples (b) and (c).

Example (a), on the other hand, has to be seen as an exception to the entire consideration given here as no consistent result for the DOS (which always includes small negative parts independent of the value for d) can be obtained with the 1D WKB model at all. To explain this result, one can either assume that the model gives no quantitatively correct description of the tunneling process in the rather complex case of a molecule adsorbed on an ultrathin insulating layer, or that the assumption of a flat tip DOS is not entirely consistent with the experimental conditions. As, however, both explanations are rather speculative, we will not give any further discussion.

After the analysis given here, two statements can be seen as evident: The 1D WKB model can be used successfully to evaluate STS $I(V)$ curves taken on organics and, by a rather simple argumentation, we found the tip-sample distance to be more likely below 5 Å for the cases studied.

Despite the remaining uncertainty in estimating a suitable value for the parameter d, we would like to point out that our

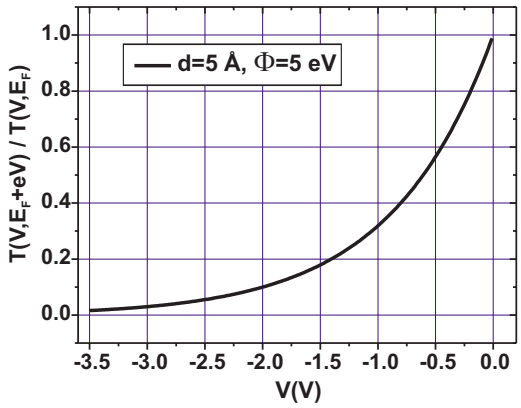

FIG. 7. (Color online) Ratio between the transmission probability at the Fermi level of the tip and at the Fermi level of the sample as a function of (negative) bias voltage. The graph can be used to estimate what fraction of the tunneling current passes through different molecular resonances.

algorithm for the DOS deconvolution is superior to existing methods, especially the simple use of the dI/dV as DOS approximation, for a number of reasons.

If the orbital-mediated tunneling process is rationalized by a combination of the 1D WKB model and additional transmission factors for each orbital which depend on the geometry of the respective orbital, both effects contribute to the measured STS $I(V)$ curve. Compared to the differential conductivity [Eq. (9)], the evaluation procedure presented here offers the possibility to eliminate the general influence of the tunneling barrier described by the 1D WKB model. This, in turn, allows us to derive quantitative information on the effects related to the orbital geometry or to level bunching as mentioned above. Such effects would otherwise only be accessible by highly sophisticated quantum chemistry calculations.[13,38] The evaluation via the 1D WKB model can further be used when the measurements are carried out with a variable tip-sample separation, thus avoiding a very complicated process including several empirical modifications.[39] Finally, it is more satisfactory from a general point of view to discuss the sample DOS as the result of a STS measurement, even if the model used for its calculation does not include all aspects of the orbital-mediated tunneling, than to discuss the dI/dV curve alone [Eq. (9)].

These conclusions can now be used to gain a valuable insight into an effect which is often said to limit the capability of STS in general.

C. Slope of T: Can deep states be probed?

It is frequently stated to be virtually impossible or at least very challenging to observe occupied sample states which are below the HOMO or the onset of the valence band in STS, as the tunneling current at negative bias is carried mainly by electrons with an energy close to the Fermi level/the upper valence band edge (in a metal/semiconductor) or by electrons in the HOMO (if molecules are involved).[26,40] This effect is attributed to the energy dependent tunneling probability $T(E)$ which favors electrons with higher energies (see Fig. 3). Although, in principle, the effect cannot be denied, our calculations indicate that it is still possible to gain information on low-lying states.

For a quantitative analysis, we plot the ratio $T(V,E_F+eV)/T(V,E_F)$ as a function of V for $d=5$ Å (Fig. 7). For a given negative voltage V_x, this quantity represents the ratio of the current through a state with an energy $E_x=E_F+eV_x$ (equals the Fermi level of the tip) to the current through a state localized at the Fermi energy (of the sample). The graph in Fig. 7 can, however, also be used to estimate the current ratio between a first state (e.g., the HOMO) at an energy $E_H<E_F$ and a second state with an energy $E_{H-1}<E_H$ at a respective bias voltage of $V_{H-1}=(E_{H-1}-E_F)/e$, which is the more relevant case for organic samples:

$$\frac{I_{H-1}}{I_H}(V_{H-1}) = \frac{T(V_{H-1},E_{H-1})}{T(V_{H-1},E_H)} \approx \left[\frac{T(V_{H-1},E_{H-1})}{T(V_{H-1},E_F)}\right] \Big/ \left[\frac{T(V_H,E_H)}{T(V_H,E_F)}\right]. \quad (14)$$

If the function in Fig. 7 is simply denoted as $y=y(V)$, the above quantity is given by $y(V_{H-1})/y(V_H)$. To give an example, the current through a state at 1 eV below E_F would, according to Fig. 7, be approximately 3.2 times higher than that through a state at 2 eV below E_F (at the relevant bias voltage of −2 V), and therefore both states should give clear fingerprints in a current-voltage measurement. We conclude that for a tip-sample distance of 5 Å or below, the slope of the transmission function is simply too small to entirely suppress the current through occupied states below the HOMO, which is the probable explanation for the significant number of experiments in which states below the HOMO could be measured successfully.[9,41,42]

As the effect which is discussed here strongly depends on T, which in turn depends on the tip-sample distance d, we suggest that a smaller tip-sample separation should generally give better access to states at lower energies. Unfortunately, the combination of a small tip-sample distance with a high bias voltage necessary to probe states far below E_F results in an extremely high tunneling current, which, in most cases, will render this approach useless from a practical point of view.

V. ROLE OF THE NORMALIZED DIFFERENTIAL CONDUCTIVITY

A. Examples and discussion

The analysis of STS evaluation procedures given in this paper would not be complete without a discussion of the ndc, a method that has first been suggested by Stroscio *et al.*[12] The original aim of the ndc was the direct comparison of STS results taken at different tip-sample separations. However, due to a number of interesting properties, the ndc rapidly became a common tool for the presentation and interpretation of STS results, thus coexisting in literature with the simple differential conductivity. Without further discussion, the method was also transferred to the case of STS on organic samples.[9,41,43,44]

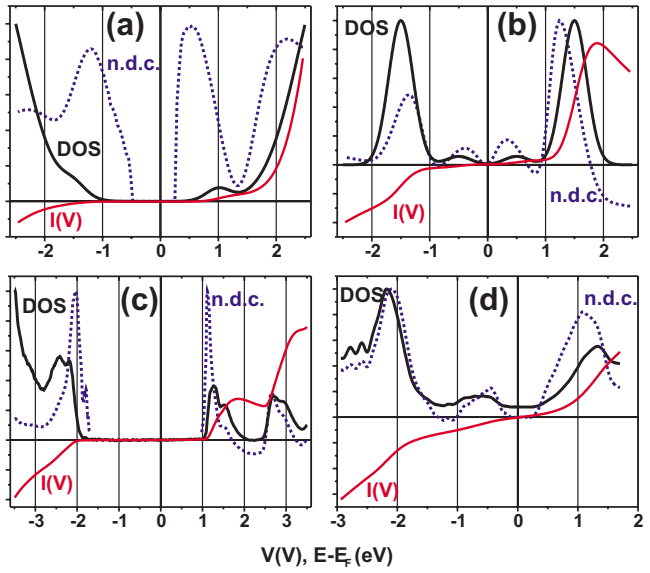

FIG. 8. (Color online) Four examples of an STS evaluation using the normalized differential conductivity. Examples (a) and (b) are evaluations of $I(V)$ curves calculated for a model DOS with the 1D WKB model (d=5 Å, Φ=5 eV). Examples (c) and (d) show real STS measurements from Grobis *et al.* (Ref. 10) and Tsiper *et al.* (Ref. 35) (see Fig. 5). The DOS shown was calculated for d =3.5 Å: (c) Φ=4.7 eV and (d) Φ=5 eV. Note that the value of the ndc always approaches unity at V=0.

The introduction of the ndc was paralleled by an analysis by Lang[19] who found that for a simple model DOS, the peak position recovered by $(dI/dV)/(I/V)$ was closer to the real values than the dI/dV peak position, thus justifying the use of the ndc. Later, the ndc was discussed in terms of the 1D WKB model by Feenstra *et al.* who concluded that it tends to cancel out the exponential dependencies of I and dI/dV on V and d.[40] The context in which the ndc is viewed is therefore rather broad. It reaches from the mentioned cancellation of exponential backgrounds[40,45] to the assumption that the ndc is a direct measure for the sample LDOS or DOS,[9,43] while a few publications also refer to the capability of the ndc to enhance features in regions with small tunneling current,[44] which is reasonable as the ndc can also be denoted as $d \ln I/d \ln V$. As we can directly calculate the DOS using the 1D WKB model, an analysis of these issues is feasible.

We abstain, however, from a detailed and exact mathematical analysis of the different properties of the ndc, but discuss two theoretical as well as two experimental examples in order to illustrate the relevant effects (Fig. 8). In all cases, the normalized differential conductivity is calculated without any empirical modification (broadening or offset[46,47]) that was developed to deal with the inherent problem of the ndc in a conductance gap, where the denominator (I/V) is close to zero. Instead, the respective part of the plot (which does not hold any information anyway) is not displayed in Fig. 8. We will now give a short analysis of the examples in Fig. 8 which are chosen to represent different scenarios.

(a) An STS measurement on a model DOS is simulated using the 1D WKB model. The DOS consists of four Gaussians: Two large peaks, centered at +3 and −3 eV, respectively, provide a background on which two (identical) smaller peaks at +1 and −1.5 eV are imposed. In a real experiment, the background might stem from several broad resonances (level bunching) outside the energy window observed. In the resulting ndc curve, the background is strongly reduced and the peaks are clearly visible; however, the position of the peaks is shifted by a rather large value of 0.5 and 0.3 eV inward if compared to the peaks in the DOS.

(b) The model DOS in the second example is similar to the one shown in Fig. 4, but with a decreased height of the inner peaks. This resembles a real STS measurement in which the contribution of HOMO and LUMO to the current is strongly suppressed for reasons (mentioned in Sec. IV B) which go beyond the 1D WKB model.[13] One finds again a strong peak shift and, in addition, the small peaks to be more accentuated in the ndc than in the DOS. This illustrates the tendency of the ndc to level the peak heights within one single measurement.

(c) For the measurement from Grobis *et al.*[10] (Fig. 5), the ndc changes the relative heights of the peaks belonging to a double peak structure drastically, while the peak positions are affected only weakly if compared to the DOS.

(d) If the ndc is calculated for the STS results from Tsiper *et al.* (Fig. 5), it shows a shift of the peak at 1.3 eV, while the −2.2 eV peak remains almost unchanged. Another effect is the change in shape of the Au(111) surface state around −0.5 V which turns from a broad feature in the DOS to a clear peak in the ndc.

These examples offer a differentiated view onto the usability of the normalized differential conductivity for the evaluation of STS $I(V)$ spectra on organics, as desired properties are paralleled especially by unwanted peak shifts. These shifts are caused by the partially extremely high slope of the normalization function (I/V) that changes at maximum by a factor of 12 in a 0.3 V region in example (c), which clearly exceeds the real slope of the transmission function (see Fig. 7). For this reason, it becomes clear that the ndc is not a useful replacement for the calculation of the DOS with the 1D WKB model in the case of organic samples. However, it cannot be denied that a subsequent normalization of the DOS can be useful in some cases, especially if peaks are hidden by a background or if they appear too weak as they contribute only weakly to the tunneling current [Figs. 8(a) and 8(b)].

In the last part of this paper, we will outline a normalization method that can be used on the DOS and which has the useful properties of the ndc, while the problematic peak shifts are avoided to a large extent.

B. Normalization method

Our aim is to develop a method that, on the one hand, reduces the influence of potential backgrounds in the DOS curve recovered and, on the other hand, emphasizes rather small peaks in regions with a low density of states. It is obviously impossible to determine the exact position of a peak with an unknown shape which is situated on a nonlinear background and thus visible as a shoulder only. As a sufficient and yet simple way to estimate the peak position, none-

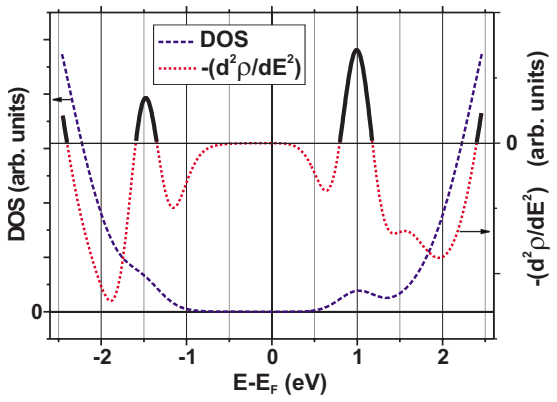

FIG. 9. (Color online) Shown is the negative second derivative of the (artificial) DOS curve from Fig. 8(a). The parts of the curve that are above zero are highlighted as they identify the two DOS peaks.

theless we propose to evaluate the second derivative of the DOS with respect to energy, which is a measure for the change in the slope of the DOS, and thus, roughly spoken, a measure for its local curvilinearity. Normally, the maximum of a peak is also the point of maximum curvilinearity, and if shoulders are considered, the x value of maximum curvilinearity is a good measure for the position of the original peak (Fig. 9).

The sign of the second derivative indicates whether the slope is increasing (positive sign) or decreasing (negative sign). The positions of peaks and shoulders in the DOS are characterized by the latter case. Therefore, we propose that DOS peaks can be identified by looking exclusively at the positive parts of the quantity $-(d^2\rho/dE^2)$ as illustrated in Fig. 9.

In order to emphasize small DOS peaks, an additional normalization of $-(d^2\rho/dE^2)$ by the DOS $\rho(E)$ seems appropriate. Therefore, we finally end up with the following quantity to evaluate:

$$-\frac{d^2\rho(E)/dE^2}{\rho(E)}. \tag{15}$$

Although peak identification is, in principle, possible using this expression, the calculation of the third derivative[48] of a measured $I(V)$ curve is not satisfactory from a practical point of view as it will, almost certainly, produce only noise. However, as we will outline here, the explicit calculation of the second derivative of the DOS can be easily avoided by applying small modifications to the concept introduced so far. First, the second derivative is expressed as central second difference quotient:

$$\frac{\rho(x+\Delta x)+\rho(x-\Delta x)-2\rho(x)}{(\Delta x)^2}. \tag{16}$$

Second, if we now drop the constant factor $(\Delta x)^2$ and use the sum of the right and left points of the interval $(x+\Delta x, x-\Delta x)$ for the normalization (rather than the central value), expression (15) can be written as

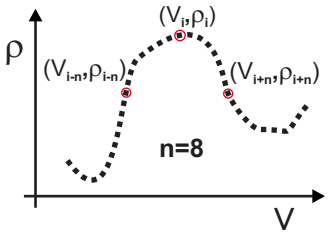

FIG. 10. (Color online) The pec algorithm normalizes a DOS value ρ_i at V_i by dividing it through $(\rho_{i-n}+\rho_{i+n})/2$.

$$\frac{2\rho(x)-[\rho(x+\Delta x)+\rho(x-\Delta x)]}{\rho(x+\Delta x)+\rho(x-\Delta x)}. \tag{17}$$

As the constant offset of -1 plays absolutely no role in finding the maxima of expression (17), we will neglect it and finally end up with:

$$\frac{2\rho(x)}{\rho(x+\Delta x)+\rho(x-\Delta x)}. \tag{18}$$

In the implementation, our method works on datasets which are given as a list of N scalar values (the DOS curve): $(V_i,\rho_i), 0<i\leqslant N$. As the main goal of the algorithm is the detection of peaks in the DOS, the result is called *peak enhanced curve* (pec). Following Eq. (18), every value ρ_i is divided through the average value of two (not necessarily closest) neighbors ρ_{i-n} and ρ_{i+n}. If ρ_i marks the center of an isolated peak, both ρ_{i-n} and ρ_{i+n} should be smaller, making $2\rho_i/(\rho_{i-n}+\rho_{i+n})>1$ (Fig. 10). The new (normalized) value at the ith data point is now found by varying n within reasonable limits while searching for the maximum:

$$\mathrm{pec}_i = \max_{0\leqslant n\leqslant n_{max}} 2\rho_i/(\rho_{i-n}+\rho_{i+n}). \tag{19}$$

As a result, two values are calculated for each DOS value ρ_i: A normalized value pec_i and the value n_i for which pec_i is maximal. The parameter n_{max} should be chosen in a way that $\Delta V = V_{i+n_{max}} - V_{i-n_{max}}$ equals approximately the width of a single peak at its base. Considering thermal broadening as well as broadening by inelastic effects, a value between 0.3 and 0.6 eV for ΔV seems reasonable. However, the functionality of the algorithm is rather tolerant with respect to the exact value of n_{max}. The lower bound of $n=0$ guarantees that pec_i will never drop below 1. To avoid unphysical peaks resulting from noisy DOS curves, it is recommended to set all pec_i values for which n_i falls below a certain threshold parameter (for example, $0.3n_{max}$) also to 1. This has the effect of a tunable filter, making further smoothing usually dispensable.

It has to be pointed out that the resulting curve is not a measure for the sample DOS anymore, but its primary aim is the identification of peaks (=molecular resonances) even if they are small or veiled by a background. The pec algorithm works rather locally as only the DOS in the interval $[V_{i-n_{max}}, V_{i+n_{max}}]$ has an influence on the normalization of ρ_i, while in the ndc the total conductivity influences the result on a global scale.[49] The functionality of the pec algorithm is illustrated for the four examples from Fig. 8 in Fig. 11. Be-

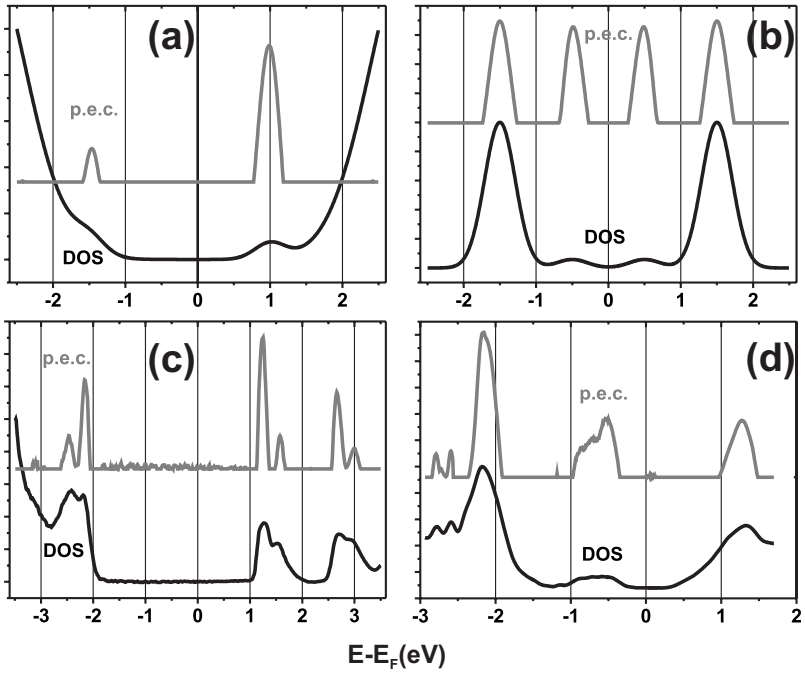

FIG. 11. Two artificial DOS curves and two DOS curves calculated from experimental measurements are evaluated with the pec algorithm. Both experimental DOS curves are recovered for d=3.5 Å and Φ=5 eV. The respective parameters for the pec are (a) ΔV=0.5 V, (b) ΔV =0.5 V, (c) ΔV=0.35 V, and (d) ΔV=0.6 V. An offset has been added to the entire DOS curve in (c) prior to the pec calculation to suppress the noise in the gap region effectively. The cutoff threshold for narrow peaks is $0.3n_{max}$ in all four cases.

sides the rather small peak shift in the pec that occurs if the peaks are highly asymmetric or only present as a shoulder, two issues are evident: The height of small peaks is indeed enhanced compared to the DOS (Ref. 50) [Figs. 11(a) and 11(b)] and the pec peaks are narrower than the peaks in the DOS. This "deconvolution" is visible especially in Fig. 11(c) where the double peak structure is clearly resolved. The background reduction as well as the narrowing of peaks can be understood if one keeps the similarity to the second derivative of the DOS in mind: Only if the first derivative is positive and decreasing or negative and increasing is the pec larger than 1.

A remaining problem is the handling of the boundary points of the (V_i, ρ_i) dataset. We choose a method that involves only a small modification, thus keeping the clear and simple functionality of the pec algorithm. The value for n_{max} is decreased for the border points in a way that $i-n_{max}>0$ as well as $i+n_{max} \leqslant N$. As a result, the first and the last points of the pec always approach 1. The detection of peaks at the very ends of the voltage range in the measurement is therefore rather difficult using the pec. However, in the examples given here, there is no peak within the range of approximately 0.3 V from the ends of the voltage range and thus the algorithm is fully usable.

VI. CONCLUSION

While the experimental method of scanning tunneling spectroscopy has successfully been extended from the investigation of inorganic samples to the investigation of thin organic layers, some specific properties of these samples, especially the rather large tunneling voltage necessary to probe the molecular resonances and the large conductance gap which is observed frequently, represent serious problems for the interpretation and understanding of such measurements. The 1D WKB model, on the other hand, is a well-known and simple description of the tunneling process which gives insight into the main properties of the elastic tunneling spectroscopy, the voltage and energy dependent transmission probability, and the tip influence. There was, however, no clear quantitative answer to the questions whether this model can also successfully be applied to STS on organics, and how strong the results are affected by the transmission function. Caused by this precariousness, the role of the normalized differential conductivity as a compensation of the transmission function was not clear as well.

After outlining the necessary steps, we have used the complete 1D WKB model to evaluate a set of STS measurements by calculating the respective sample DOS. Following a simple argumentation based on the assumption of an entirely positive DOS and a relative symmetry in the height of DOS peaks at positive and negative voltages, we found that the tunneling barrier parameters d and Φ have comparable and physically meaningful values for the examples investigated. We could, however, show that it is impossible to determine both values exactly and independently. Nevertheless, the 1D WKB model can be applied to three of the four cases investigated, and by inductive reasoning we conclude that it is a suitable method for the evaluation of STS results on organics in general. The parameters that have been found for the tunneling barrier allow us to estimate the contribution of molecular resonances below the HOMO to the tunneling current. According to our results, the contribution cannot be neglected, thus supporting the idea that these resonances can be observed in STS, indeed.

For a number of examples, we have compared the calculated DOS curves to the normalized differential conductivity of the respective $I(V)$ curve, thus checking the different properties and functionalities that are attributed to this evaluation method. Although, according to our results, the ndc cannot be seen as a direct measure for the sample DOS, and

despite the occurrence of significant peak shifts, the ndc nevertheless exhibits interesting and useful properties. As the ndc can therefore be merely seen as a mathematical method to detect peaks, we have outlined a different method that has the useful properties of the ndc but avoids strong peak shifts and that can be used on the DOS after the recovery with the 1D WKB model.

Note added in proof. Recently, we became aware that somewhat similar results were published by Koslowski *et al.*[54] Note that they also discuss an approach to the calculation of the DOS by exploiting the 1D WKB model and Volterra equations, but that there is no discussion on the implications for scanning tunneling spectroscopy on *organic* nanolayers, which is the major aim of our paper.

ACKNOWLEDGMENT

Financial support by the Deutsche Forschungsgemeinschaft (DFG) Grants No. FR875/6-1, No. FR875/6-2, and No. FR875/9-1 is gratefully acknowledged.

*Electronic address: wagner@iapp.de. URL: http://www.iapp.de

[1] G. Binnig, H. Rohrer, C. Gerber, and E. Weibel, Phys. Rev. Lett. **49**, 57 (1982).
[2] C. W. Tang and S. A. VanSlyke, Appl. Phys. Lett. **51**, 913 (1987).
[3] Q. Huang, K. Walzer, M. Pfeiffer, V. Lyssenko, G. He, and K. Leo, Appl. Phys. Lett. **88**, 113515 (2006).
[4] C. W. Tang, Appl. Phys. Lett. **48**, 183 (1986).
[5] J. Drechsel, B. Maennig, F. Kozlowski, M. Pfeiffer, K. Leo, and H. Hoppe, Appl. Phys. Lett. **86**, 244102 (2005).
[6] A. Aviram and M. A. Ratner, Chem. Phys. Lett. **29**, 277 (1974).
[7] C. Joachim, J. K. Gimzewski, and A. Aviram, Nature (London) **408**, 541 (2000).
[8] Often, those states are not quite correctly called "orbitals" as well.
[9] M. Toerker, T. Fritz, H. Proehl, R. Gutierrez, F. Grossmann, and R. Schmidt, Phys. Rev. B **65**, 245422 (2002).
[10] M. Grobis, A. Wachowiak, R. Yamachika, and M. F. Crommie, Appl. Phys. Lett. **86**, 204102 (2005).
[11] J. Tersoff and D. R. Hamann, Phys. Rev. Lett. **50**, 1998 (1983).
[12] J. A. Stroscio, R. M. Feenstra, and A. P. Fein, Phys. Rev. Lett. **57**, 2579 (1986).
[13] P. Sautet and M.-L. Bocquet, Phys. Rev. B **53**, 4910 (1996).
[14] M. Magoga and C. Joachim, Phys. Rev. B **59**, 16011 (1999).
[15] A. I. Onipko, K.-F. Berggren, Y. O. Klymenko, L. I. Malysheva, J. J. W. M. Rosink, L. J. Gerrligs, E. van der Drift, and S. Radelaar, Phys. Rev. B **61**, 11118 (2000).
[16] J. J. W. M. Rosink, M. A. Blauw, L. J. Geerligs, E. van der Drift, and S. Radelaar, Phys. Rev. B **62**, 10459 (2000).
[17] The Wentzel-Kramers-Brillouin approximation or semiclassical approximation is applicable if the change in the potential $U(x)$ is small at the scale of the wavelength of Ψ.
[18] A. Selloni, P. Carnevali, E. Tosatti, and C. D. Chen, Phys. Rev. B **31**, 2602 (1985).
[19] N. D. Lang, Phys. Rev. B **34**, 5947 (1986).
[20] J. Bardeen, Phys. Rev. Lett. **6**, 57 (1961).
[21] For a different approach see, for example, Ref. 51.
[22] Approximately 10 meV (Ref. 23).
[23] J. Tersoff and D. R. Hamann, Phys. Rev. B **31**, 805 (1985).
[24] For a simple tip model, such calculations can be found in Refs. 51 and 52.
[25] To highlight this analogy, not only the tip-sample distance d from Fig. 2 is used in Eq. (4) but $r_0=d+R$.
[26] V. A. Ukraintsev, Phys. Rev. B **53**, 11176 (1996).
[27] J. Repp, G. Meyer, S. M. Stojković, A. Gourdon, and C. Joachim, Phys. Rev. Lett. **94**, 026803 (2005).
[28] A comparable calculation was performed by Hamers for an STS measurement on Si(111)-(7×7) without giving details on the procedure used (Ref. 53).
[29] For a different approach, see Ref. 15.
[30] *Surveys on Solution Methods for Inverse Problems*, edited by D. Colton, H. Engl, A. Louis, J. McLaughlin, and W. Rundell, (Springer-Verlag, Vienna/New York, 2000), p. 68.
[31] P. Linz, Comput. J. **12**, 393 (1969).
[32] Such a possibility was considered by Ukraintsev (Ref. 26) but our results contradict this conclusion.
[33] This becomes trivial in the limit of $d=0$ where the calculated DOS equals dI/dV which is inevitably negative in a NDR region.
[34] D. E. Barlow, L. Scudiero, and K. W. Hipps, Langmuir **20**, 4413 (2004).
[35] E. Tsiper, Z. Soos, W. Gao, and A. Kahn, Chem. Phys. Lett. **360**, 47 (2002).
[36] N. Nicoara, O. Custance, D. Granados, J. M. García, J. M. Gómez-Rodríguez, A. M. Baró, and J. Méndez, J. Phys.: Condens. Matter **15**, 2619 (2003).
[37] I. Hill, A. Kahn, J. Cornil, D. dos Santos, and J. Bredas, Chem. Phys. Lett. **317**, 444 (2000).
[38] C. L. Kane, E. J. Mele, A. T. Johnson, D. E. Luzzi, B. W. Smith, D. J. Hornbaker, and A. Yazdani, Phys. Rev. B **66**, 235423 (2002).
[39] R. M. Feenstra, Phys. Rev. B **50**, 4561 (1994).
[40] R. M. Feenstra, J. A. Stroscio, and A. P. Fein, Surf. Sci. **181**, 295 (1987).
[41] C. Baldacchini, C. Mariani, M. G. Betti, L. Gavioli, M. Fanetti, and M. Sancrotti, Appl. Phys. Lett. **89**, 152119 (2006).
[42] M. Takada and H. Tada, Jpn. J. Appl. Phys., Part 1 **44**, 5332 (2005).
[43] R. Strohmaier, C. Ludwig, J. Petersen, B. Gompf, and W. Eisenmenger, Surf. Sci. **351**, 292 (1996).
[44] P. G. Collins, J. C. Grossman, M. Côté, M. Ishigami, C. Piskoti, S. G. Louie, M. L. Cohen, and A. Zettl, Phys. Rev. Lett. **82**, 165 (1999).
[45] W. Deng and K. W. Hipps, J. Phys. Chem. B **107**, 10736 (2003).
[46] P. Mårtensson and R. M. Feenstra, Phys. Rev. B **39**, 7744 (1989).
[47] M. Prietsch, A. Samsavar, and R. Ludeke, Phys. Rev. B **43**, 11850 (1991).
[48] In this simplified view, the calculation of the DOS is seen as the first derivative.
[49] Example: While the outcome of the pec algorithm is not affected by the width of a conductance gap, the total conductivity and thus the ndc are.

[50] Changes in the relative height of the peaks can be made if an offset is added to the entire curve prior to the pec calculation.
[51] F. R. Zypman and L. F. Fonseca, Phys. Rev. B **55**, 15912 (1997).
[52] F. R. Zypman, L. F. Fonseca, and Y. Goldstein, Phys. Rev. B **49**, 1981 (1994).
[53] R. J. Hamers, *Scanning Tunneling Microscopy and Spectroscopy: Theory, Techniques, and Applications* (Wiley-VCH, Weinheim, 1993), Chap. 4, pp. 75–80.
[54] B. Koslowski, C. Dietrich, A. Tschetschetkin, and P. Ziemann, Phys. Rev. B **75**, 035421 (2007).